Hindawi Publishing Corporation
International Journal of Polymer Science
Volume 2015, Article ID 176826, 11 pages
http://dx.doi.org/10.1155/2015/176826

Research Article

Prediction of Mold Spoilage for Soy/Polyethylene Composite Fibers

Chinmay Naphade,[1] Inyee Han,[2] Sam Lukubira,[3] Amod Ogale,[3] James Rieck,[4] and Paul Dawson[2]

[1]*Farbest Foods, Jasper, IN 47546, USA*
[2]*Food, Nutrition and Packaging Sciences, Clemson University, Clemson, SC 29634, USA*
[3]*Chemical and Biomolecular Engineering, Clemson University, Clemson, SC 29634, USA*
[4]*Department of Mathematics, Clemson University, Clemson, SC 29634, USA*

Correspondence should be addressed to Paul Dawson; pdawson@clemson.edu

Received 1 September 2014; Accepted 19 December 2014

Academic Editor: Long Yu

Mold spoilage was determined over 109 days on soy/PE fibers held under controlled temperatures (T) ranging from 10°C to 40°C and water activities (a_w) from 0.11 to 0.98. Water activities were created in sealed containers using saturated salt solutions and placed in temperature-controlled incubators. Soy/PE fibers that were held at 0.823 a_w or higher exhibited mold growth at all temperatures. As postulated, increased water activity (greater than 0.89) and temperature (higher than 25°C) accelerated mold growth on soy/PE fibers. A slower mold growth was observed on soy/PE fibers that were held at 0.87 a_w and 10°C. A Weibull model was employed to fit the observed logarithmic values of T, a_w, and an interaction term $\log T \times \log a_w$ and was chosen as the final model as it gave the best fit to the raw mold growth data. These growth models predict the expected mold-free storage period of soy/PE fibers when exposed to various environmental temperatures and humidities.

1. Introduction

Natural/biofiber composites are emerging as a viable alternative to glass fiber composites, particularly in automotive, packaging, building, and consumer product industries becoming one of the fastest growing additives for thermoplastics. Biocomposites can mimic the structures of living materials by providing strengthening properties to the matrix while still providing biocompatibility, for example, in creating scaffolds in bone tissue engineering [1] (Kispotta and Bisoyi, 2011). Biocomposites are composite materials that contain one or more phase(s) derived from a biological origin [2]. For biocomposites the reinforcement could be fibers like cotton, flax, hemp, wood, or even by-products from food crops. Matrices may be polymers, ideally derived from renewable resources such as vegetable oils or starches. One of the most commonly used matrices is synthetic, fossil-derived polymers. Biocomposites integrate "soft" biological and organic molecular assemblies with "hard" inorganic nanoarchitectures combining materials having disparate chemical and physical properties within a single system.

The addition of natural fillers or reinforcements is postulated to lower the manufacturing cost and increase the stiffness of composites [3]. Fillers also provide advantages of lower energy consumption and faster cycle time during production. Another major advantage of these reinforcements is incorporation of biopolymers such as starches and proteins into composites enhancing degradation of plastic materials [4].

Several studies have reported on the incorporation of biopolymers, such as starch and protein, into extrusion blown polyethylene films [5, 6]. Films combining protein with synthetic plastics show potential for production of compostable plastic materials. Degradation of proteins by microorganisms can render the remaining synthetic polymer vulnerable to photodegradation or thermal degradation.

Gurram et al. (2002) [7] studied the properties of wood, soy hull fiber, and big blue stem on the tensile and flexural properties of fibers. They found that Young's modulus of wood, big blue stem, and soy hull fiber composites were comparable to pure polypropylene and polyethylene. These researchers also concluded that biorenewable fibers such as soybean hulls could be used as reinforcing materials for low cost composites and that environmental and energy savings benefits could be another advantage of biocomposites. Zhang et al. (1999) [8] studied biocomponent fibers that were wet-spun from soybean protein and poly(vinyl alcohol) for textile applications. They determined that the protein core of the spun biocomponent fiber was brittle and showed a high frequency of core breakage upon drawing. Thus an effort was made to investigate the soybean protein solution, with the aim of trying to understand the cause for fiber brittleness and to determine the optimum solution conditions for fiber spinning.

Ghorpade et al. (1995) [9] evaluated the cast forming ability of soy protein isolates with varying amounts of polyethylene oxides (PEO) and determined that addition of PEO decreased film tensile strength (TS) and increased elongation at break (E). Scanning electron micrographs of film cross-sections showed a decrease in positive texture attributes with increasing amounts of PEO in the films. Jong (2005) [10] used defatted soy flour (DSF) for rubber reinforcements. The reinforcement mechanism of DSF in rubber used carboxylated polystyrene-butadiene as a composite matrix and was characterized by static and dynamic mechanical methods. These results indicated that DSF was a more effective option than either soy protein isolate or concentrate in terms of both mechanical properties and cost.

The growth of microorganisms like bacteria or molds on a substrate is governed by the intrinsic and extrinsic factors [11, 12]. Following are the important intrinsic factors:

(i) moisture content,

(ii) nutrient content,

(iii) oxidation-reduction potential (Eh)

(iv) pH.

Extrinsic factors influencing microbial growth are

(i) temperature,

(ii) relative humidity,

(iii) presence and concentration of gases,

(iv) presence and activities of other microorganisms.

Mold can grow on many surfaces where oxygen and moisture are present. Biocomposites are more susceptible to microbial growth than fossil-derived polymers due to their hydrophilic nature and nutrient availability. Moisture sorption isotherms have been studied for a range of biological materials including starch powders [13, 14], pasta [15], tea leaves [16], corn stover [17], alfalfa cubes [18], oats/oatmeal biscuits [19], bean flour [20], and cookies [21]. Moisture sorption isotherms have also been used to study bio-based films formed from starch [22], whey protein [23], chicken feather keratin [24], and zein [25]. Models predicting mold growth under various moisture conditions have also been developed [26].

Igathinathane et al. (2008) [27] developed a model to predict the storage life of corn stover components without mold growth when exposed to different temperature and humidity conditions. In order to maintain humidity conditions, saturated salts solutions were placed in temperature controlled chambers. The desiccators were used to create environments having temperatures from 10°C to 40°C and a_w of 0.11 to 0.98. At a high water activity (>0.90 a_w) and a temperature of 30°C, mold growth occurred in corn leaf, stalk, and skin rapidly. One-, two-, and three-parameter models were assessed for their performance to predict mold-free days (MFDs) based on temperature and a_w. The three-parameter model gave the best prediction compared to the exponential model. The single parameter $T \times a_w$ product model produced slightly better results than the two-parameter model. Three-parameter model featured all parameters and the t-statistics revealed that the combined $T \times a_w$ product variable was more significant than variables of T and a_w. They concluded that a predictive model could be utilized to predict the safe storage period of corn stover components under controlled temperature and a_w conditions.

Various authors [28–30] reviewed different mathematical isotherm models that can be used to predict the stability of biological materials. Though several articles have been studied, there is no single model identified that can describe the sorption characteristics of soy composites. Thus, the objective of the present study was to develop statistical model to predict mold-free shelf life of soy/PE based as influenced by temperature and water activity.

2. Materials and Methods

2.1. Production of Soy/PE Fibers. Soy flour, grade of 7B2, was provided by ADM (Archer Daniels Midland Company, USA). Linear low density PE, ASPUN grade, was provided by Dow Chemicals (Bristol, Pennsylvania). All fibers were produced at Clemson University Chemical and Biomolecular Engineering. Soy/PE fibers were produced using a proprietary blending of defatted soy flour, a spun pure PE pellets, and a compatibilizer. These materials were blended together using a DSM compounder twin screw microextruder (Xplore Pharma, RD Geleen, Netherlands), to obtain dispersion of soy particles in PE phase. The blended materials were further extruded using a pilot scale single screw extruder (Alex James & Associates, Greenville, SC) to melt spin soy/PE fibers and pure PE fibers. Pellets were fed to single screw extruder that was designed to deliver molten soy/PE mixture at constant pressure to the melting pump. The extruder die had three 500 micron diameter openings to extrude fibers. Fibers were then spun on a continuously spinning unit with a take-up of specific revolutions per minutes (rpm), reducing fiber diameter. This process yielded consistent fibers having a diameter of 50–100 microns, which were further spun on a clean spool.

2.2. Saturated Salt Solutions. Individual containers (16 ounce pint Mason Jars, Ball, Rome, Georgia) were used to hold fiber

Table 1: Water activity of saturated salt solutions at five different temperatures.

Saturated salt solution	Water activity				
	10°C	25°C	30°C	35°C	40°C
Lithium chloride	0.113	0.113	0.113	0.113	0.112
Potassium acetate	0.234	0.225	0.216	0.216	0.216
Magnesium chloride	0.335	0.328	0.324	0.321	0.316
Potassium carbonate	0.431	0.432	0.432	0.41	0.40
Sodium bromide	0.622	0.576	0.560	0.546	0.532
Sodium chloride	0.757	0.753	0.751	0.749	0.747
Potassium chloride	0.868	0.843	0.836	0.830	0.823
Potassium nitrate	0.960	0.936	0.923	0.908	0.890
Potassium sulfate	0.982	0.973	0.970	0.967	0.964

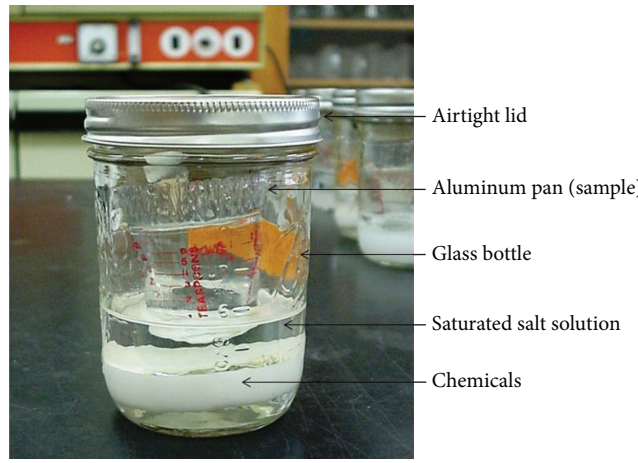

Figure 1: Experimental setup for establishing different water activities in containers using different saturated salt solutions. One gram of soy/PE fiber sample was placed in each jar in aluminum pans.

samples. The various water activities were created by the addition of nine different salts (lithium chloride, potassium acetate, magnesium chloride, potassium carbonate, sodium bromide, sodium chloride, potassium chloride, potassium nitrate, and potassium sulfate) in 70 mL of nanopure water until each solution was saturated. Salts and water solutions were vigorously agitated using magnetic stirrer to facilitate saturation. Additional salt was added as initially added salts dissolved in water to maintain saturation. Saturated salt solutions were placed in temperatures of 10, 25, 30, 35, and 40°C. Once saturated salt solutions became temperature equilibrated, a_w ranging from 0.11 to 0.98 was generated depending upon the salt and temperature combination (Table 1).

2.3. Sample Preparation. Soy/PE and pure PE fibers were carefully removed from the spool using sterile gloves as received from production. 1.000 g of fiber was weighed on a digital balance with a sensitivity of 0.0001 g. Fiber samples were prepared from soy/PE fiber spool and stored in a sterile glass holder. Fiber samples were weighed and all necessary information such as initial weight before drying, final weight after drying, and the sample number was marked onto the glass holders. Samples were loaded into a convection oven (Thelco Laboratory Oven 130DM, Precision Scientific, Chicago, Illinois) at 55°C for 15 hrs to equilibrate fiber moisture content to <0.1%. Fibers were then held in a desiccator for 1 hr to cool. Fiber samples were reweighed placed in a sterilized aluminum pans and were randomized using random number generator statistical software [31] (SAS 9.3, 2012).

Initially fiber samples that were predried were placed in nine different salt solution containers (Figure 1) at temperatures of 10, 25, 30, 35, and 40°C (Gravity Convection Incubator 1.1CF120, VWR, Atlanta, GA). Water activities ranged from 0.11 to 0.98 depending upon the salt and temperature combination. Soy/PE fiber samples were placed in all the above-mentioned conditions for 50 days to examine the range of water activity at which mold spoilage was observed on soy/PE fibers. The experiment was run twice independently with a fresh spool of soy/PE fiber for each replication. Fibers that were stored in high a_w (in a range of 0.8–0.98) exhibited mold growth and hence a separate experiment (that was replicated 3 times) was conducted to develop a model that could precisely predict the onset of mold growth in soy/PE fibers.

2.4. Experimental Setup. 30 soy/PE fiber samples placed in the desiccator for 1 hr were reweighed in aluminum pans before they were loaded into saturated salt solution containers. Before loading into saturated salt solution containers, soy/PE fiber samples were randomized as mentioned above in sample preparation. Weighing process was critical and hence was carried out quickly as fibers were dry in nature and long-term exposure to laboratory air could have led to reabsorption of moisture. A one ounce small glass (Anchor Hocking number 82412) was placed into the saturated solution with an aluminum pan containing fiber sample carefully positioned on the glass (Figures 2(a), 2(b), and 2(c)). This arrangement avoided any contact of aluminum pan with the saturated salt solution. Lids were opened daily and the fiber samples were thoroughly inspected for any possible visual signs of mold growth and fiber sample weights were monitored regularly until fibers had attained equilibrium moisture content (EMC). The moisture content of the product in equilibrium with air is known as EMC and the relative humidity of the air as equilibrium relative humidity (ERH) [32]. Crystalline thymol is commonly used in moisture sorption studies as an antimicrobial to prevent microbial spoilage at very high relative humidity and was not used in this study.

Soy/PE fiber samples were stored at five different temperature-controlled incubators (10, 25, 30, 35, and 40°C) (Gravity Convection Incubator 1.1CF120, VWR, Atlanta, GA, USA). At each temperature setting, 6 fiber samples were held in 3 different saturated solutions (KCl, KNO_3, and K_2SO_4) creating a_w ranges of 0.823–0.868, 0.890–0.960, and 0.964–0.982. Each of the 6 fiber samples was placed in separate saturated solution containers to reduce contamination of mold spores from one sample to another.

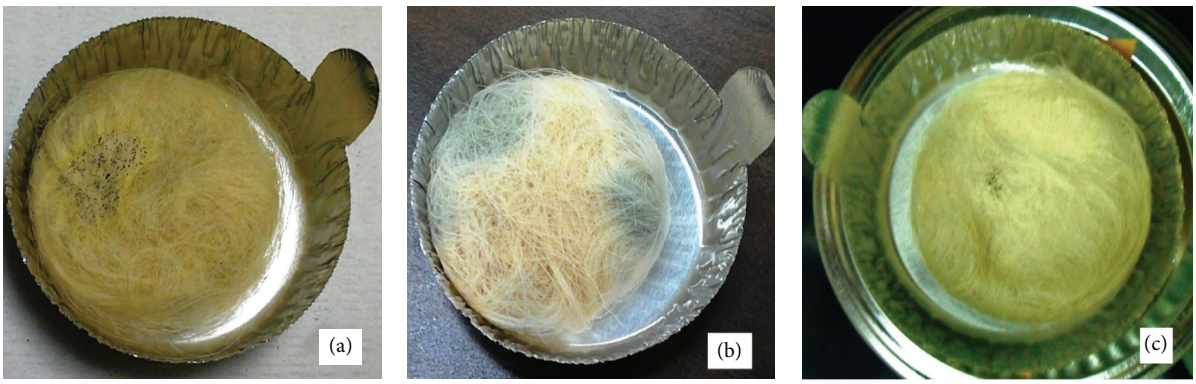

Figure 2: One gram of soy/PE fiber sample in aluminum pans that developed mold spoilage. (a) Mold spores, (b) visible mold mycelium when placed in high humidity environments, and (c) mold growth on fibers with an area approximately 5% of total area that was termed as positive mold spoilage for modeling purposes.

2.5. Calculations of Mold-Free Days. Mold growth was regularly monitored on fibers by visual examination. Visible spores and subsequent germ tube development from the spores into a radiating system of hyphae known as mycelium (white to greenish cloudy appearance) were an indication of mold spoilage on the fiber surfaces. Fiber surfaces demonstrating equivalent or more than 5% surface area covered with mold (spores or mycelium) were termed as positive for mold spoilage (Figure 2(c)). Without the aid of magnifying lenses, the smallest object humans can resolve approximately 100 μm or 0.1 mm in diameter, which is approximately the size of a fine pencil dot [33]. Therefore, this is the range of mold colony size that could first be observed in this study. Elapsed days until the day of first mold appearance in the form of black dots or visible network of mycelium (Figure 2) was observed and was designated as mold-free days (MFDs) for modeling purposes. Mathematically, MFD is one less than the days counted to the first mold appearance [11]. Moisture absorbed in fibers during experiments was calculated from the initial and final sample weights. Weight gained by soy/PE fibers was monitored regularly. The experiment was replicated 3 times using a fresh spool of soy/PE fiber for each replicate.

2.6. Model Development and Selection. The number of MFDs under specific temperature and water activity conditions can vary from one replicate to another. Thus, MFD is a random variable that has a probability distribution. This probability distribution also affected temperature and a_w for which a model was developed to account for these effects.

In this study, several probability distributions with a location and a scale parameter were considered to represent the distribution of MFDs. These distributions included the normal, lognormal, and Weibull distributions. The regression model assumes that the location parameter is a linear function of independent variables. Candidate independent variables for this study included the temperature (T), water activity (A), the interaction of temperature and water activity (TA) and the transformations of the logarithm (base 10) of temperature (LT), the logarithm of water activity (LA) and the interaction of the logarithm of temperature, and the logarithm of water activity (LTLA).

For all three distributions, the following candidate sets of independent variables were used for the regression model of the location parameter: (T), (A), (TA), (T, A), (T, TA), (A, TA), (T, A, TA), (LT), (LA), (LTLA), (LT, LA), (LT, LTLA), (LA, LTLA), and (LT, LA, LTLA). The LIFEREG procedure from SAS was used to obtain the maximum likelihood estimates for the scale parameter and the regression coefficients for all the candidate sets of independent variables.

Model selection criteria such as Akaike information criterion (AIC) and Akaike information criterion correction (AICc) can be used to choose among the various distributions and sets of independent variables. The AIC provides an estimate of the expected Kullback-Leibler information that measures the information loss when the current model is used to approximate the "true" model that generated the data. Thus models with small AIC values are preferred since less information is lost. The AIC is calculated by

$$\mathrm{AIC} = -2\log(\mathscr{L}) + 2K, \tag{1}$$

where ($\mathscr{L}$) is the maximized likelihood of a fitted model and (K) is the number of free parameters in the model itself. When the sample size (n) is small with respect to the maximum K in the set (approximately $n/K < 40$), AIC is no longer adequate. A better estimate is provided by AICc which provides a finite sample correction for the Akaike information criterion. The AICc can be calculated by

$$\mathrm{AICc} = -2\log(\mathscr{L}) + 2K\left(\frac{n}{(n-K-1)}\right). \tag{2}$$

The Δ_i statistic of a model i in a model set is simply

$$\Delta_i = \mathrm{AIC}_i - \mathrm{AIC}_{\min}, \tag{3}$$

where $\mathrm{AIC}_{\min}$ is the minimum value of AIC in the set (hence, $\Delta_i = 0$ for the best model). Models with Δ_i less than approximately 8–12 have essentially no support, those in which $4 \le \Delta_i \le 7$ have considerably less support, models with Δ_i between 0 and 4 receive considerable support from the current data, and models with Δ_i in the 0–2 range perform virtually as well as the best model in the set [34].

Burnham and Anderson (2002) [35] strongly recommend using AICc rather than AIC, if n is small or K is large. For this study, the AICc was calculated for each candidate distribution and set of independent variables. In addition, pseudo R^2 for the models was estimated using the likelihood ratio [36]. The pseudo R-squared is calculated as follows:

$$R^2 = 1 - \exp\left[\frac{(x_2 - x_1)}{n}\right], \quad (4)$$

where R^2 is pseudo R-squared value, $x_1 = -2$Log Likelihood (model with no independent variables), $x_2 = -2$Log Likelihood (current model), and n is sample size.

The predicted values of MFDs from the chosen model were obtained for the all the temperatures (ranging from 10°C to 40°C) and a_w (ranging 0.80 to 1.00). A 3D surface plot was developed for predicted MFD values for a_w (0.80–1.00) and temperature (10°C–40°C) using MATLAB software (R2012B, The MathWorks, Natick, MS). The observed values of MFDs from all three replications were then mapped on the 3D surface model from all replications to establish the prediction efficacy of the best chosen model. A precise mapping of the observed values of MFDs on the 3D surface suggests prediction capability of the optimal model superior to that of the other chosen models.

3. Results and Discussion

Soy/PE fibers placed in a_w environments ranging from 0.112 to 0.982 at five different temperatures (10°C, 25°C, 30°C, 35°C, and 40°C) for 50 days developed mold growth only at the higher a_w (0.8–0.98) levels. Hence a separate experiment was implemented to determine a best suited model using SAS 9.3 and develop a 3D plot using MATLAB software to predict mold growth on fibers exposed to temperature and humidity conditions under which mold growth developed after 50 days.

Soy/PE fibers held with saturated potassium chloride solutions (0.868–0.823 a_w) absorbed the least moisture (in a range of 0.0329–0.0631 g) (Figure 3) and hence a slower mold growth in fibers was observed. For fiber samples held with potassium chloride solutions (0.868 a_w), ones held at 10°C had the greatest MFDs (101–108) compared to fibers held under other temperatures. Fibers held with potassium chloride solutions (0.868–0.823 a_w) at 25°C, 30°C, 35°C, and 40°C had MFDs in a range of 38–52 (Table 2).

Soy/PE fibers held with potassium nitrate solutions (0.890–0.960 a_w) absorbed moisture in a range of 0.0594–0.1473 g (Figure 4). Soy/PE fibers held at 0.960 a_w and 10°C had MFDs of 38–40, while fibers held with potassium nitrate solutions (0.890–0.936 a_w) and kept at 25, 30, 35, and 40°C had MFDs in a range of 6–14 (Table 2).

Soy/PE fiber samples held with potassium sulfate solutions (0.964–0.982 a_w) absorbed moisture in the range of 0.1564–0.237 g (Figure 5). The potassium sulfate solution yielded the highest water activity 0.982 at 10°C resulting in MFDs of 32–34, while fibers held with the same salt solution at 25, 30, 35, and 40°C with 0.964–0.973 a_w had MFDs in a range of 4–10 (Table 2). Thus, soy/PE fibers were comparatively less stable to mold growth and can display

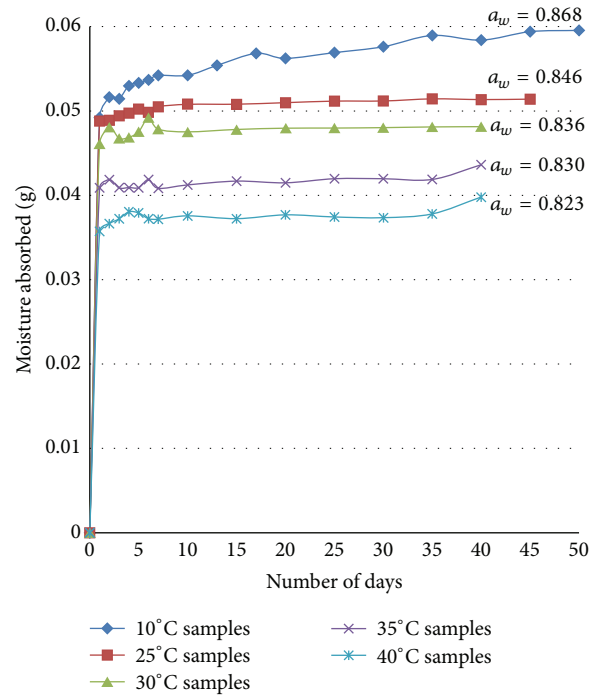

Figure 3: Soy/PE fiber samples stored with potassium chloride salt solutions at different temperatures (10°C, 25°C, 30°C, 35°C, and 40°C). Ultimate moisture absorbed during storage in different a_w (0.868, 0.846, 0.836, 0.830, and 0.823, respectively). Each data point denotes a mean value of 6 samples in 3 replications.

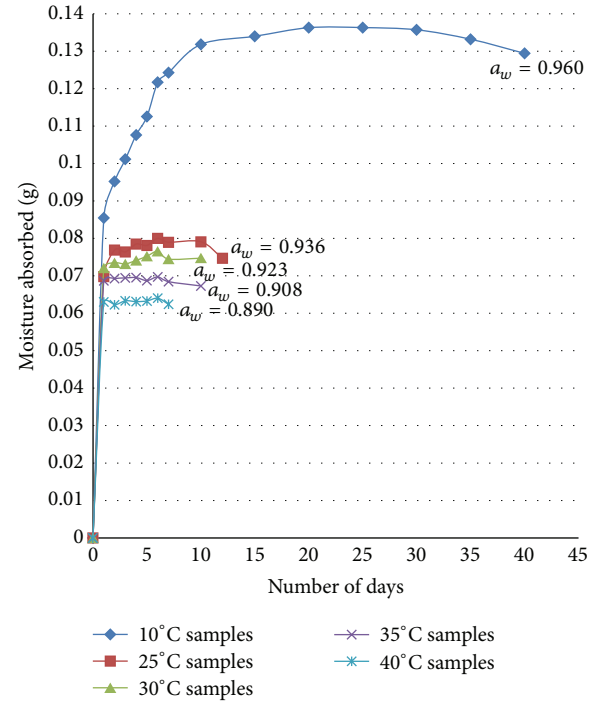

Figure 4: Soy/PE fiber samples stored with potassium nitrate salt solutions at different temperatures (10°C, 25°C, 30°C, 35°C, and 40°C). Ultimate moisture absorbed during storage in different relative humidities (0.960, 0.936, 0.923, 0.908, and 0.890, respectively). Each data point denotes a mean value of 6 samples in 3 replications.

Table 2: Mold-free days (MFD) for soy/PE fiber samples held at different temperatures and water activities.

Temperature (T) in °C	Water activity (a_w)	Replication 1		Replication 2		Replication 3		Average	$T \times a_w$
		MFD	Final moisture content	MFD	Final moisture content	MFD	Final moisture content	MFD	
10	0.868	105	0.055	101	0.0631	99	0.0566	102	8.68
	0.868	106	0.0578	108	0.0596	102	0.0589	105	8.68
	0.96	40	0.1212	40	0.1473	38	0.1346	39	9.6
	0.96	40	0.1248	39	0.1423	39	0.1295	39	9.6
	0.982	34	0.2258	32	0.2329	32	0.2322	33	9.82
	0.982	33	0.2302	33	0.237	32	0.2275	33	9.82
25	0.843	52	0.0461	49	0.0578	49	0.0529	50	21.08
	0.843	51	0.0457	49	0.0573	50	0.0499	50	21.08
	0.936	13	0.0742	13	0.0857	14	0.0777	13	23.40
	0.936	12	0.0752	14	0.081	13	0.0789	13	23.40
	0.973	10	0.1896	9	0.2192	8	0.2008	9	24.33
	0.973	9	0.1956	9	0.2218	9	0.1945	9	24.33
30	0.836	49	0.0451	45	0.0533	43	0.047	46	25.08
	0.836	48	0.044	45	0.0529	42	0.0468	45	25.08
	0.923	10	0.0717	12	0.0775	11	0.0748	11	27.69
	0.923	9	0.0721	12	0.0783	12	0.0739	11	27.69
	0.97	8	0.1701	8	0.1879	8	0.1763	8	29.10
	0.97	8	0.1682	8	0.1905	8	0.1734	8	29.10
35	0.83	44	0.0401	43	0.0465	40	0.0392	42	29.05
	0.83	43	0.039	42	0.0489	40	0.0382	42	29.05
	0.908	8	0.0672	10	0.0724	10	0.0678	9	31.78
	0.908	8	0.0652	10	0.071	11	0.0673	10	31.78
	0.967	7	0.1627	7	0.1697	6	0.162	7	33.85
	0.967	7	0.1629	6	0.1742	6	0.1665	6	33.85
40	0.823	41	0.0378	40	0.0421	38	0.0347	40	32.92
	0.823	41	0.0381	40	0.0412	38	0.0329	40	32.92
	0.89	6	0.0642	7	0.0688	7	0.0594	7	35.60
	0.89	7	0.0606	7	0.0659	7	0.062	7	35.60
	0.964	5	0.1618	4	0.1657	5	0.1572	5	38.56
	0.964	5	0.1611	5	0.1646	5	0.1564	5	38.56

mold growth before 10 days when temperatures are ≥25°C and ≤40°C and a_w is in a range of 0.964–0.973. Fibers did not have mold growth for 3 days under the most extreme (high temperature, high a_w) conditions tested (Figure 6).

Fiber samples stored at all a_w and placed in 25, 30, 35, and 40°C incubators absorbed maximum moisture within 2 days and subsequently a slight increase or retention of moisture was observed over the time of study. A gradual increase in moisture content was observed in fiber samples stored at all a_w at 10°C. However, fiber samples stored in highest a_w (0.964–0.982) and placed in 25, 30, 35, and 40°C initially absorbed more moisture as compared to fibers stored at 10°C. Hence, it may be concluded that temperature and rate of moisture absorption accelerated mold growth in soy/PE fibers kept at 25, 30, 35, and 40°C compared to 10°C. Temperature also affects the growth rate with the optimum growth temperature between 30 and 40°C.

For the first replicate, the three models that possessed the smallest AICc values for the Weibull distribution were the (LT, LA), (LT, $LTLA$), and (LT, LA, $LTLA$) models (Table 3). The AICc values were 175.654, 172.341, and 173.439, respectively. Since the difference in the AICc values among the three models was less than 3 there is no preference among these models. For the second replicate, the three models that possessed the smallest AICc values for the Weibull distribution were again the (LT, LA), (LT, $LTLA$), and (LT, LA, $LTLA$) models (Table 3). The AICc values were 160.645, 155.6, and 155.235, respectively. Since the difference in the AICc values for the (LT, LA) model is over 5 compared to the other two models, it was not chosen as a preferred model. There was no preference between the (LT, $LTLA$) and the (LT, LA, $LTLA$) models. For the third replicate, the three models that possessed the smallest AICc values for the Weibull distribution continued to be the (LT, LA),

Table 3: LIFEREG procedure analysis in SAS 9.3 using lognormal and Weibull distribution utilizing observed logarithmic values of T, a_w, and a logarithmic interaction term of $LT \times La_w$ and MFD in three individual replications.

Distribution	n	Model	AICc	$-2\ln(\mathscr{L})$	Pseudo R-squared
			Values from Experiment 1		
Lognormal	30	*LTLA*	256.404	249.481	0.226
Lognormal	30	*LT*, *LA*	187.678	178.078	0.929
Lognormal	30	*LT*, *LTLA*	186.637	177.037	0.931
Lognormal	30	*LA*, *LTLA*	233.236	223.636	0.673
Lognormal	30	*LT*, *LA*, *LTLA*	188.727	176.227	0.933
Lognormal	30	None	261.616	257.171	0
Weibull	30	*LTLA*	263.024	256.101	0.140
Weibull	30	*LT*, *LA*	175.654	166.054	0.957
Weibull	30	*LT*, *LTLA*	172.341	162.741	0.962
Weibull	30	*LA*, *LTLA*	240.402	230.802	0.630
Weibull	30	*LT*, *LA*, *LTLA*	173.439	160.939	0.964
Weibull	30	None	265.086	260.641	0
			Values from Experiment 2		
Lognormal	30	*LTLA*	254.99	248.067	0.215
Lognormal	30	*LT*, *LA*	173.822	164.222	0.961
Lognormal	30	*LT*, *LTLA*	172.053	162.453	0.953
Lognormal	30	*LA*, *LTLA*	230.366	220.766	0.784
Lognormal	30	*LT*, *LA*, *LTLA*	173.648	161.148	0.961
Lognormal	30	None	260.7	256.256	0
Weibull	30	*LTLA*	262.011	255.088	0.119
Weibull	30	*LT*, *LA*	160.645	151.045	0.979
Weibull	30	*LT*, *LTLA*	155.6	146	0.974
Weibull	30	*LA*, *LTLA*	237.922	228.322	0.758
Weibull	30	*LT*, *LA*, *LTLA*	155.235	142.735	0.979
Weibull	30	None	263.902	259.458	0
			Values from Experiment 3		
Lognormal	30	*LTLA*	235.626	228.703	0.230
Lognormal	30	*LT*, *LA*	148.411	138.811	0.962
Lognormal	30	*LT*, *LTLA*	152.244	142.644	0.956
Lognormal	30	*LA*, *LTLA*	201.617	192.017	0.773
Lognormal	30	*LT*, *LA*, *LTLA*	151.25	138.75	0.962
Lognormal	30	None	241	236.556	0
Weibull	30	*LTLA*	243.242	236.319	0.135
Weibull	30	*LT*, *LA*	131.432	121.832	0.981
Weibull	30	*LT*, *LTLA*	132.69	123.09	0.980
Weibull	30	*LA*, *LTLA*	211.692	202.092	0.724
Weibull	30	*LT*, *LA*, *LTLA*	132.079	119.579	0.982
Weibull	30	None	245.123	240.679	0

(*LT*, *LTLA*), and (*LT*, *LA*, *LTLA*) models (Table 3). The AICc values were 131.432, 132.69, and 132.079, respectively. Since the difference in the AICc values for the (*LT*, *LA*), (*LT*, *LTLA*), and the (*LT*, *LA*, *LTLA*) models is the same, there was no preference between the (*LT*, *LA*), (*LT*, *LTLA*), and the (*LT*, *LA*, *LTLA*) models.

The three replications were successfully converged into one and the three models that possessed the smallest AICc values for the Weibull distribution were the (*LT*, *LA*), (*LT*, *LTLA*), and (*LT*, *LA*, *LTLA*) models. The AICc values were 454.527, 447.77, and 441.685, respectively. The model (*LT*, *LA*, *LTLA*) was the best suited model among the chosen sets and was determined based on the least AICc number and highest pseudo R^2 value (0.974) (Table 4). Δ_i for the (*LT*, *LA*, *LTLA*) model would be zero. Since the Δ_i for the (*LT*, *LA*) model is over 12 compared to (*LT*, *LA*, *LTLA*) model and Δ_i for the (*LT*, *LTLA*) model is over 6 compared to (*LT*, *LA*, *LTLA*) model, those models were not chosen as preferred models.

Thus the (*LT*, *LA*, *LTLA*) model was a preferred model for all three replicates and the final converged replicate and

Table 4: LIFEREG procedure analysis in SAS 9.3 using normal, lognormal, and Weibull distribution utilizing observed logarithmic values of T, a_w, and a logarithmic interaction term of $LT \times La_w$ and MFD by converging all three replications together.

Distribution	n	Model	AICc	$-2\ln(\mathscr{L})$	Pseudo R-squared
Normal	90	T	795.929	789.65	0.304
Normal	90	TA	777.768	771.489	0.431
Normal	90	A	794.574	788.295	0.315
Normal	90	T, TA	722.94	714.47	0.698
Normal	90	T, A, TA	641.592	630.877	0.881
Normal	90	T, A	664.946	656.476	0.842
Normal	90	A, TA	675.076	666.606	0.823
Normal	90	None	826.443	822.305	0
Lognormal	90	T	721.653	715.374	0.319
Lognormal	90	TA	696.565	690.286	0.485
Lognormal	90	A	714.953	708.674	0.368
Lognormal	90	T, A	513.004	504.533	0.935
Lognormal	90	T, A, TA	501.898	491.183	0.944
Lognormal	90	T, TA	534.015	525.544	0.918
Lognormal	90	A, TA	503.76	495.289	0.941
Lognormal	90	None	754.145	750.007	0
Lognormal	90	LT	720.065	713.786	0.331
Lognormal	90	$LTLA$	732.591	726.312	0.231
Lognormal	90	LA	714.13	707.851	0.374
Lognormal	90	LA, $LTLA$	649.852	641.381	0.701
Lognormal	90	LT, LA, $LTLA$	491.783	481.069	0.949
Lognormal	90	LT, $LTLA$	494.044	485.574	0.947
Lognormal	90	LT, LA	494.084	485.613	0.947
Lognormal	90	None	754.145	750.007	0
Weibull	90	LT	737.865	731.586	0.278
Weibull	90	$LTLA$	753.965	747.686	0.137
Weibull	90	LA	735.125	728.846	0.299
Weibull	90	LA, $LTLA$	672.841	664.371	0.658
Weibull	**90**	**LT, LA, LTLA**	**441.685**	**430.971**	**0.974**
Weibull	90	LT, LA	454.527	446.057	0.969
Weibull	90	LT, $LTLA$	447.77	439.299	0.972
Weibull	90	None	765.045	760.907	0

hence it was chosen as the final model. The data from all three replicates were pooled and each replicate was treated as a random effect for the location parameter and the final maximum likelihood estimates for the scale and location parameters were determined using the NLMIXED procedure from SAS 9.3 (SAS, 2012). The maximum likelihood estimate of the scale parameter is given by

$$\widehat{\sigma} = 0.1193. \tag{5}$$

The maximum likelihood estimate for the location parameter is given by the following equation:

$$\begin{aligned}\widehat{\mu} = {} & 6.8216 - 1.5294\mathrm{Log}_{10}(T) - 4.6835\mathrm{Log}_{10}(A) \\ & - 2.1739\mathrm{Log}_{10}(T) \times \mathrm{Log}_{10}(A).\end{aligned} \tag{6}$$

The maximum likelihood estimate of the $100 \times p$ percentile of mold-free days is given by

$$\mathrm{MFD}_p = \exp\left(\widehat{\mu} + \widehat{\sigma}\ln\left[-\ln\left(1-p\right)\right]\right). \tag{7}$$

For example, to estimate the median number of mold-free days, p is 0.5.

The pseudo R-squared for the model is 0.974 (Table 4).

A 3D surface was developed using values obtained from converged replications (i.e. predicted values of MFDs for an entire set of temperatures (10°C–40°C) and water activity (0.80–1.00)) (Figures 6(a) and 6(b)). The observed MFD values from all the three replications were then mapped on the 3D surface of the model derived from all replications. These MFD values appeared on the 3D surface plot with no or very little deviation for the model (Figure 6(b)). It was

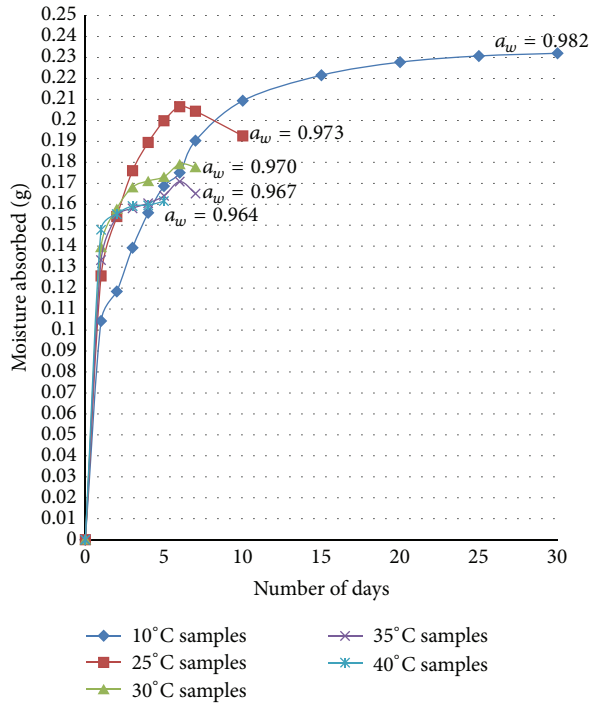

FIGURE 5: Soy/PE fiber samples stored with potassium sulfate salt solutions at different temperatures (10°C, 25°C, 30°C, 35°C, and 40°C). Ultimate moisture absorbed during storage in different relative humidities (0.982, 0.973, 0.970, 0.967, and 0.964, respectively). Each data point denotes a mean value of 6 samples in 3 replications.

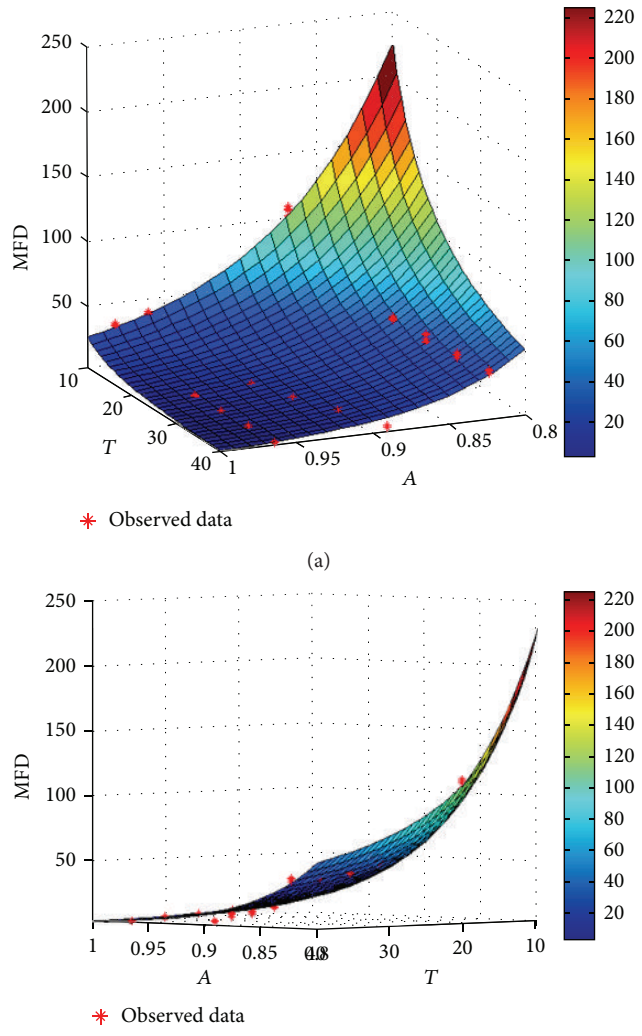

FIGURE 6: (a) Prediction model for the median number of mold-free days (MFDs) based on temperature (T) and water activity (A) values obtained from the Weibull distribution utilizing observed logarithmic values of T, a_w, and an interaction term of $T \times a_w$ of three replications. Observed mold growth expressed as mold-free days (MFDs) on soy/PE fiber samples from all three replications shown as points on the graph to demonstrate the relationship of observed values to the predicted values. (b) A side-view of (a).

concluded that the selected model was effective for predicting MFDs at given temperatures (10°C–40°C) and a_w (0.80–1.00 a_w) (Figures 6(a) and 6(b)). Mold growth on biocomposite films is more likely compared to petroleum-based films due to the availability of nutrients and moisture. Iganthinathane et al. (2008) [27] modeled the MFDs to predict the safe storage time and conditions for corn stover reporting that the product of storage temperature and storage a_w was simple predictor of mold-free days. This only held for the present study for similar a_w at different temperatures (Table 2). When a greater number of temperatures and a_w were tested, predicting the growth of mold was not as straightforward. The current study demonstrates a method to predict mold growth and permit the safe storage of soy-PE composites. The current model predicts over 200 MFDs when stored at 80% RH (0.8 a_w) and 10°C. Similar models could be used to predict MFDs for the bio-based fibers to create safe storage periods and conditions for biocomposites.

Films combining protein with synthetic plastics show potential for production of compostable plastic materials. In particular, nonwoven products are replacing many woven and knit materials because they are low in cost and are lightweight. Degradation of bio-based components by microorganisms can render the remaining synthetic polymer vulnerable to photodegradation or thermal degradation. While the use of biocomposites can be expanded to produce highly functional, inexpensive material, the need for testing to determine stability will be required due to the degradability of the biological component. The methods and results reported here predict the stability bio-based composites and can be used to develop stable biocomposites in the future.

Conflict of Interests

The authors declare that there is no conflict of interests regarding the publication of this paper.

Acknowledgment

This research was partially supported by a Grant from the United Soybean Board (USB), Grant no. 1480 and 9480 "Continuous Calendering-Extrusion Route: Melt-Processing

of Ribbon-Fiber Based Nonwovens and Films Derived from Soy Proteins."

References

[1] U. G. Kispotta and D. K. Bisoyi, *Synthesis and characterization of bio-composite material [Master of Science in Physics]*, National Institute of Technology, Rourkela. India, 2011.

[2] P. A. Fowler, J. M. Hughes, and R. M. Elias, "Biocomposites: technology, environmental credentials and market forces," *Journal of the Science of Food and Agriculture*, vol. 86, no. 12, pp. 1781–1789, 2006.

[3] K. C. Oksman and C. Clemons, "Mechanical properties and morphology of impact modified polypropylene-wood flour composites," *Journal of Applied Polymer Science*, vol. 67, no. 9, pp. 1503–1513, 1998.

[4] G. J. L. Griffin, "Biodegradable fillers in thermoplastic," in *Fillers and Reinforcements for Plastics*, R. D. Deanin and N. R. Schott, Eds., vol. 134 of *Advances in Chemistry Series*, pp. 159–170, American Chemical Society, Washington, DC, USA, 1974.

[5] V. M. Ghorpade and M. A. Hanna, "Physical and mechanical properties of soy protein isolate-polyethylene extrudates," ASAE Paper 93-6533, American Society of Agricultural Engineers, Chicago, Ill, USA, 1993.

[6] H. J. Park, J. M. Bunn, R. F. Testin, P. J. Vergano, and D. D. Edie, "Characteristics of corn zein filled polyethylene films," Tech. Rep. 822, IFT, Chicago, Ill, USA, 1993.

[7] S. Gurram, J. L. Julson, K. Muthukumarrapan, D. D. Stokke, and A. K. Mahapatra, "Application of bio renewable fibers in composites," in *Proceedings of the ASAE/CSAE North Central Intersectional Conference*, 2002.

[8] Y. S. Zhang, S. Ghasemzadeh, A. M. Kotliar, S. Kumar, S. Presnell, and L. D. Williams, "Fibers from soybean protein and poly(vinyl alcohol)," *Journal of Applied Polymer Science*, vol. 71, no. 1, pp. 11–19, 1999.

[9] V. M. Ghorpade, A. Gennadios, M. A. Hanna, and C. L. Weller, "Soy protein isolate/poly(ethylene oxide) films," *Cereal Chemistry*, vol. 72, no. 6, pp. 559–563, 1995.

[10] L. Jong, "Characterization of defatted soy flour and elastomer composites," *Journal of Applied Polymer Science*, vol. 98, no. 1, pp. 353–361, 2005.

[11] J. M. Jay, M. J. Loessner, and D. A. Golden, *Modern Food Microbiology*, Springer, New York, NY, USA, 7th edition, 2005.

[12] W. C. Frazier and D. C. Westhoff, *Food Microbiology*, McGraw-Hill, New York, NY, USA, 3rd edition, 1988.

[13] A. H. Al-Muhtaseb, W. A. M. McMinn, and T. R. A. Magee, "Water sorption isotherms of starch powders: part 1: mathematical description of experimental data," *Journal of Food Engineering*, vol. 61, no. 3, pp. 297–307, 2004.

[14] A. H. Al-Muhtaseb, W. A. M. McMinn, and T. R. A. Magee, "Water sorption isotherms of starch powders. Part 2: thermodynamic characteristics," *Journal of Food Engineering*, vol. 62, no. 2, pp. 135–142, 2004.

[15] M. Erbaş, M. F. Ertugay, and M. Certel, "Moisture adsorption behaviour of semolina and farina," *Journal of Food Engineering*, vol. 69, no. 2, pp. 191–198, 2005.

[16] H. M. Ghodake, T. K. Goswami, and A. Chakraverty, "Moisture sorption isotherms, heat of sorption and vaporization of withered leaves, black and green tea," *Journal of Food Engineering*, vol. 78, no. 3, pp. 827–835, 2007.

[17] C. Igathinathane, A. R. Womac, S. Sokhansanj, and L. O. Pordesimo, "Sorption equilibrium moisture characteristics of selected corn stover components," *Transactions of the American Society of Agricultural Engineers*, vol. 48, no. 4, pp. 1449–1460, 2005.

[18] M. H. Khoshtaghaza, S. Sokhansanj, and B. D. Gossen, "Quality of Alfalfa cubes during shipping and storage," *Applied Engineering in Agriculture*, vol. 15, no. 6, pp. 671–676, 1999.

[19] W. A. M. McMinn, D. J. McKee, and T. R. A. Magee, "Moisture adsorption behaviour of oatmeal biscuit and oat flakes," *Journal of Food Engineering*, vol. 79, no. 2, pp. 481–493, 2007.

[20] N. D. Menkov, A. G. Durakova, and A. Krasteva, "Moisture sorption isotherms of common bean flour at several temperatures," *Electronic Journal of Environmental, Agricultural and Food Chemistry*, vol. 4, no. 2, pp. 892–898, 2005.

[21] E. Palou, A. López-Malo, and A. Argaiz, "Effect of temperature on the moisture sorption isotherms of some cookies and corn snacks," *Journal of Food Engineering*, vol. 31, no. 1, pp. 85–93, 1997.

[22] T. Chowdhury and M. Das, "Moisture sorption isotherm and isosteric heat of sorption characteristics of starch based edible films containing antimicrobial preservative," *International Food Research Journal*, vol. 17, no. 3, pp. 601–614, 2010.

[23] S.-J. Kim and Z. Ustunol, "Solubility and moisture sorption isotherms of whey-protein-based edible films as influenced by lipid and plasticizer incorporation," *Journal of Agricultural and Food Chemistry*, vol. 49, no. 9, pp. 4388–4391, 2001.

[24] S. M. Martelli, G. Moore, S. S. Paes, C. Gandolfo, and J. B. Laurindo, "Influence of plasticizers on the water sorption isotherms and water vapor permeability of chicken feather keratin films," *LWT-Food Science and Technology*, vol. 39, pp. 292–301, 2006.

[25] Y. Wang and G. W. Padua, "Water sorption properties of extruded *Zein* films," *Journal of Agricultural and Food Chemistry*, vol. 52, no. 10, pp. 3100–3105, 2004.

[26] R. F. LeBouf, S. A. Schuckers, and A. Rossner, "Preliminary assessment of a model to predict mold contamination based on microbial volatile organic compound profiles," *The Science of the Total Environment*, vol. 408, no. 17, pp. 3648–3653, 2010.

[27] C. Igathinathane, A. R. Womac, L. O. Pordesimo, and S. Sokhansanj, "Mold appearance and modeling on selected corn stover components during moisture sorption," *Bioresource Technology*, vol. 99, no. 14, pp. 6365–6371, 2008.

[28] J. Chirife and H. A. Iglesias, "Equations for fitting water sorption isotherms of food: part 1—a review," *International Journal of Food Science & Technology*, vol. 13, no. 3, pp. 159–174, 1978.

[29] C. van den Berg and S. Bruin, "Water activity and its estimation in food systems—theoretical aspects," in *Water Activity: Influences on Food Quality*, L. B. Rockland and G. F. Stewart, Eds., pp. 1–61, Academic Press, New York, NY, USA, 1981.

[30] N. Wang and J. G. Brennan, "Moisture sorption isotherm characteristics of potatoes at four temperatures," *Journal of Food Engineering*, vol. 14, no. 4, pp. 269–287, 1991.

[31] SAS Institute, *SAS Software.Version [9.3]*, SAS Institute, Cary, NC, USA, 2012.

[32] D. R. Heldman, *Encyclopedia of Agricultural, Food, and Biological Engineering*, Marcel Dekker, New York, NY, USA, 2003.

[33] G. Saladin, *Anatomy and Physiology: The Unity of Form and Function*, McGraw-Hill, New York, NY, USA, 2004.

[34] A. E. Raftery, "Bayesian model selection in social research," *Sociological Methodology*, vol. 25, pp. 111–163, 1995.

[35] K. P. Burnham and D. R. Anderson, *Model Selection and Multimodel Inference: A Practical Information-Theoretic Approach*, Springer, 2nd edition, 2002.

[36] L. Magee, "R^2 measures based on Wald and likelihood ratio joint significance tests," *The American Statistician*, vol. 44, no. 3, pp. 250–253, 1990.